Article
Vol. 23, No. 2, p. 299–314, April 2019
https://doi.org/10.1007/s12303-018-0039-7
pISSN 1226-4806 eISSN 1598-7477
Geosciences Journal GJ

Hydrochemical equilibrium and statistical approaches as effective tools for identifying groundwater evolution and pollution sources in arid areas

Mohamed El Alfy[1,2]*, Fathy Abdalla[3,4], Karim Moubark[4], and Talal Alharbi[5]

[1]Prince Sultan Institute for Environmental, Water and Desert Research, King Saud University, Riyadh, PO Box 2454, 11451, Saudi Arabia
[2]Geology Department, Faculty of Science, Mansoura University, Mansoura, Dakahlia Governorate 35516, Egypt
[3]Deanship of Scientific Research, King Saud University, Riyadh, PO Box 2454, 11451, Saudi Arabia
[4]Geology Department, Faculty of Science, South Valley University, Qena, Qena Governorate 83523, Egypt
[5]Geology Department, Faculty of Science, King Saud University, Riyadh, PO Box 2454, 11451, Saudi Arabia

ABSTRACT: Hydrochemical investigations, including geochemical analyses, multivariate statistics and geostatistics, were conducted to assess the factors that influence groundwater geochemistry and pollution potentiality in Luxor area, Upper Egypt. A total of thirty-one groundwater and surface water samples from the Quaternary aquifer and the River Nile were analyzed for fourteen physical and chemical variables for each sample. Spatial variations in total dissolved solids and nitrate concentration were mapped. Piper and Durov diagrams indicate that the hydrochemistry of groundwater is influenced by the secondary processes; mixing with fresh water from the River Nile and El Kalabia Canal, irrigation return flow, and sewage leakage, and reverse ion-exchange process. The hydrochemical modeling of mineral phase saturation indices shows that nearly all of the groundwater points are undersaturated with reference to calcite, aragonite, dolomite, anhydrite, gypsum, and halite. Correlation coefficients of the different variables are consistent with the saturation indices. Cluster analysis was used to identify four significant, distinct groundwater zones where the original groundwater was influenced differently by mixing processes. Factor analysis showed four mutually interfering factors reveal the chemical characteristics of the groundwater; these factors are caused by rock-water interactions, mixing of waters of different origins, and anthropogenic effects. Integration of hydrochemical and statistical analyses approach can be applied for the better management of water resources at a regional scale and in areas with comparable conditions.

Key words: factor and cluster analyses, saturation indices, groundwater pollution, Luxor area

Manuscript received October 9, 2017; Manuscript accepted May 16, 2018

1. INTRODUCTION

In arid areas, groundwater is an important and precious resource; in the Luxor area, Egypt, it represents the second source of water for agricultural, municipal, and industrial supplies. Increasing demand for and usage of water, particularly groundwater, greatly increase the risk of overuse and contamination. Groundwater quality in this region has been deteriorated due to interactions with aquifer minerals and anthropogenic influences; therefore, understanding the hydrogeochemical aspects that affect groundwater geochemistry and quality is crucial. Factors that affect groundwater chemistry include composition of precipitation, geological structures, mixing process, ion exchange, redox, leaching, and dissolution (El Alfy et al., 2015). The interactions of these factors generate various water facies (Thivya et al., 2014). The water quality parameters for the chemical stability of groundwater include temperature, alkalinity, calcium concentration, pH and total dissolved solids (TDS). Adverse impacts of water corrosion can be manifest in borehole and well equipment failures, pump failures, clogging of well screens, and damage to pipes used for urban water distribution.

Natural systems are generally more complex than first anticipated; therefore, it can be challenging to consider all relevant variables to influence hydrochemistry. Without adequate understanding of all relevant features together, interpretation is significantly impeded. Multivariate statistics, such as cluster and

*Corresponding author:
Mohamed El Alfy
Prince Sultan Institute for Environmental, Water and Desert Research, King Saud University, Riyadh, PO Box 2454, 11451, Saudi Arabia
Tel: +966-1-4699812, Fax: +966-1-4675574, E-mail: melalfy@ksu.edu.sa

factor analyses, can examine the natural and anthropogenic factors that influence water geochemistry (El Alfy, 2013). Factor analysis is a promising method for interpreting groundwater hydrochemical data and connecting them to specific geochemical processes. It is also used as a classification tool for determining water facies and origins (Lawrence and Upchurch, 1982). The main objectives of this research are to identify the evolution of groundwater quality and hydrochemistry in Luxor area, Upper Egypt. To investigate these hydrochemical trends, various geochemical calculations have been performed including hydrochemical investigations, multivariate statistical and geostatistical analyses techniques.

1.1. Study Area

The study area is located in the Luxor governorate, Upper Egypt; it has an area of 104 km^2 (Fig. 1). This arid area has dry and hot conditions with average temperature ranges between 23 C (winter) and 44 C (summer). Although annual rainfall is less than 5 mm/y, episodic flash showers happen during winter and spring. The evapotranspiration rate is about 185 cm/y, the annual mean wind speed is 4.06 m/s, and the relative humidity ranges from 53% (in winter) to 29% (in summer) (Abdalla et al., 2009).

1.2. Geology and Hydrogeology

The area of study is characterized by a succession of Upper Cretaceous, Tertiary and Quaternary sedimentary rock (Fig. 2); the oldest locally exposed units are Eocene in age (Said, 1981; Omran et al., 2001). The Quaternary deposits are made up of silt, sand, gravel, and conglomerate. The Pliocene sediments were formed by aggradation and degradation of the Nile Valley (Ezz El Deen et al., 2013). The Eocene Thebes Formation is made up of largely massive limestone intercalated with silt and clay. The upper Paleocene includes the Dakhla Formation and the Tarawan Chalk, which are characterized by shale and marl,

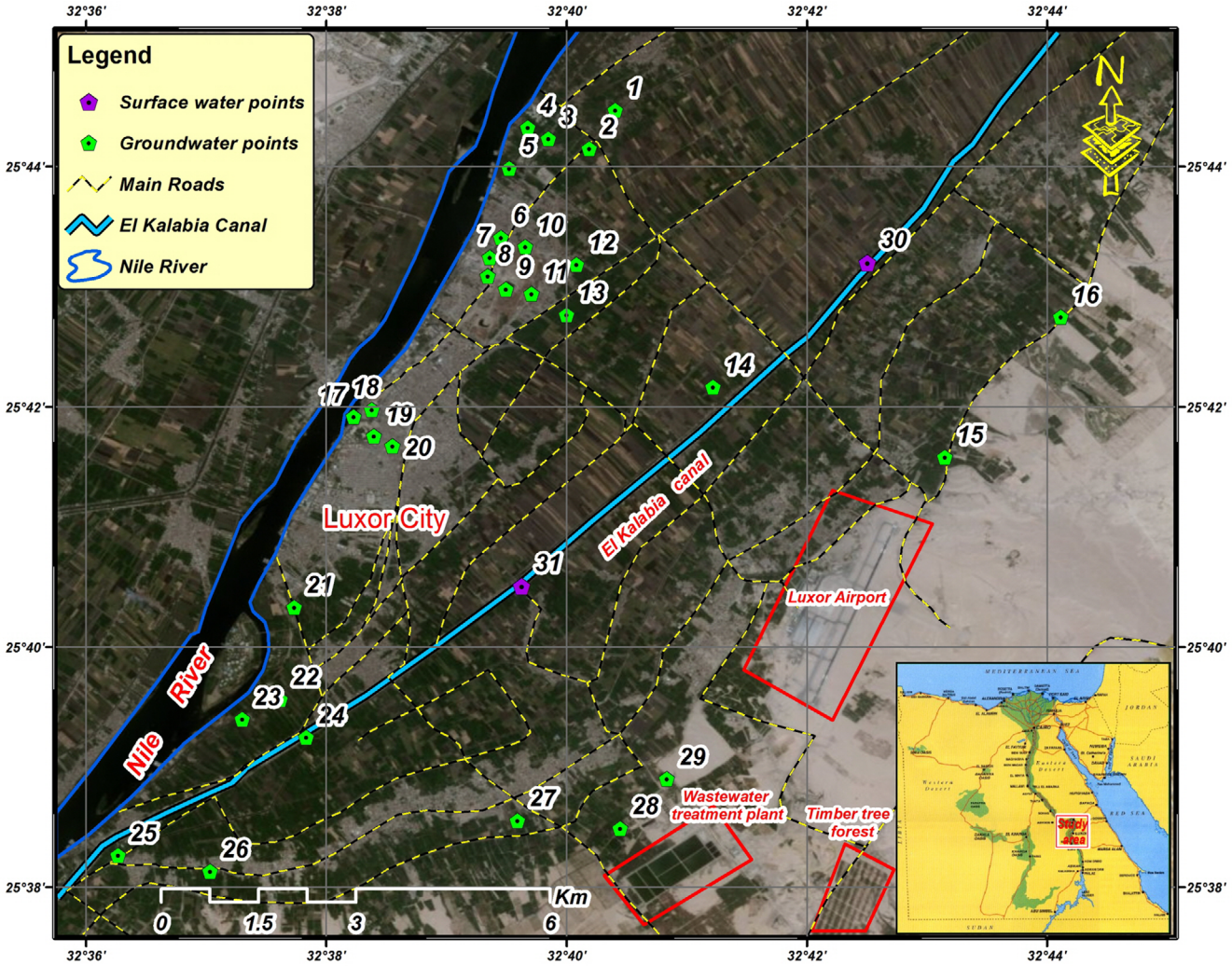

Fig. 1. Location map showing the sampled water points.

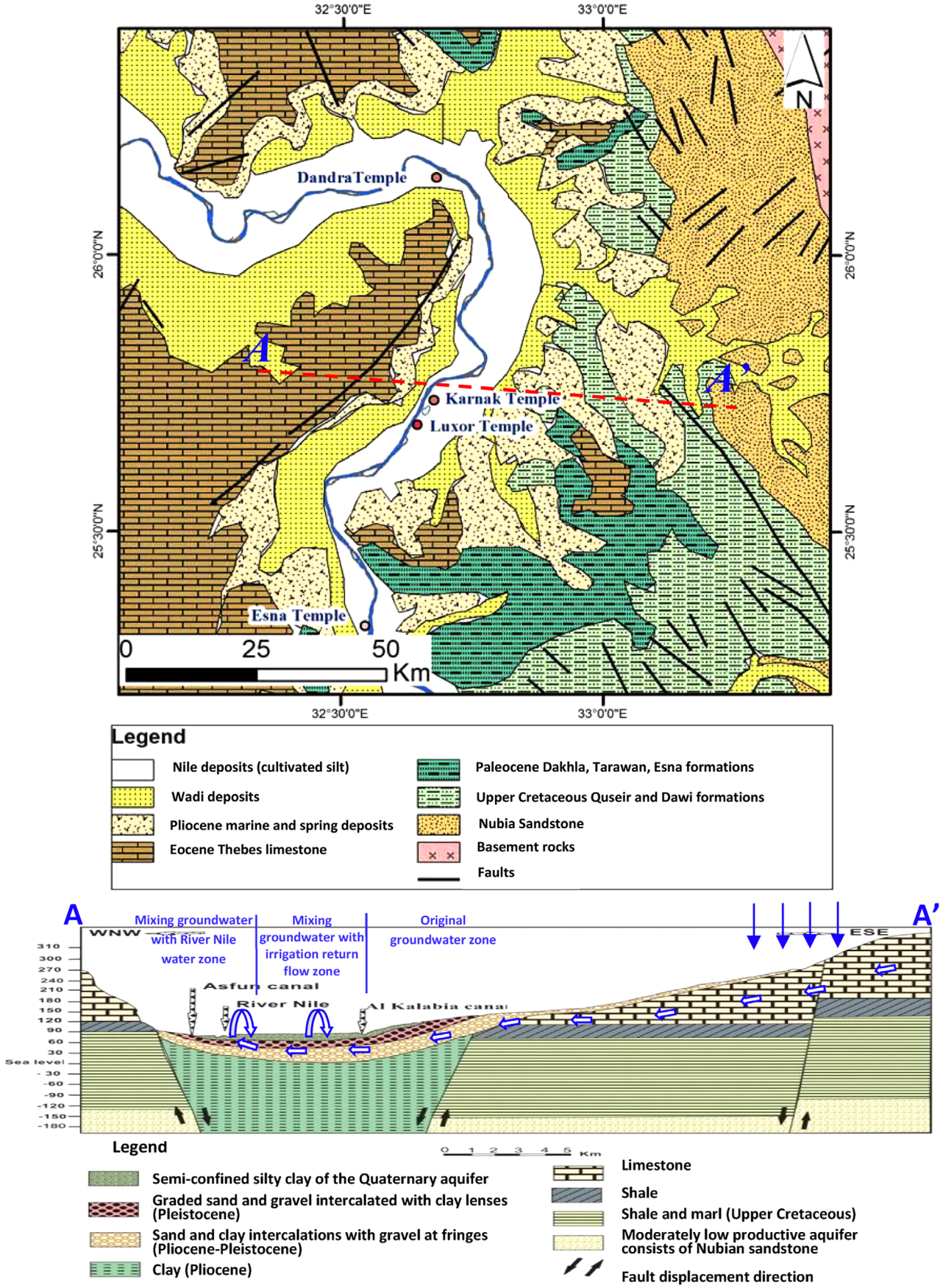

Fig. 2. Geology of the study area and its surroundings (after EGSM, 1981) with the hydrogeological cross-section A–A' (modified from RIGW, 1997).

https://doi.org/10.1007/s12303-018-0039-7

whereas the lower Paleocene is made up of the Esna Shale. The Dakhla Formation of the Upper Cretaceous includes sand, shale, marl, and limestone underlain by the phosphates of the Duwi Formation (Ezz El Deen et al., 2013).

In the study area, the surface water system includes the River Nile, irrigation canals, and agricultural drains. The minimum water discharge of the River Nile from the Aswan High Dam is 75 10^6 m^3/day (January), whereas its maximum discharge is 240 10^6 m^3/day (August) (Abd El-Bassier, 1997). The El Kalabia irrigation canal extends along the study area. Water for the canal is directly provided by the River Nile. It extends approximately 270 km with a maximum water level upstream of 71.8 m amsl (July and August), and 66 m amsl (January). The El Kalabia canal is used to irrigate an area of about 480 km^2 with a maximum discharge of 88.5 10^6 m^3/day (July and August), and a minimum discharge of 41.5 10^6 m^3/day (January).

The hydrogeological system of the study area is a part of the Nile Valley Quaternary aquifer. This aquifer is divided into two main hydrogeological units; the Holocene aquitard that is composed of clay, silty-clay, and clayey-silt deposits, and the Pleistocene aquifer of graded sand and gravel with clayey lenses intercalations. The Pleistocene aquifer is underlain by Pliocene clays that are generally considered to form the impervious base of the aquifer. The Holocene aquitard thickness varies between 12.5 m and 26 m (Abdalla et al., 2009), it receives surface water seepage, which accumulates as subsoil water. The horizontal and vertical permeability of this unit increase with depth and vary between 0.40 to 1.00 m/day (Abd El-Monim, 1986). The Pleistocene aquifer, which the River Nile cuts through, is highly productive, and the groundwater exists under semi-confined conditions. The aquifer thickness decreases from 300 m (Sohag) to a few tens of meters (southwest of Luxor) (Sayed, 2004). The aquifer hydraulic conductivity varies between 60 to 100 m/day, and the transmissivity between 2,000 and 6,000 m^2/day (Attia, 1985). Overall, the groundwater flows north, although local trends occur with flow moving either toward or away from the River Nile. The regional piezometry indicates groundwater flow is toward the River Nile, which acts as a major natural drain. The lateral flow from the River Nile into the aquifer has been demonstrated upstream of the Esna barrages (Moubark, 2013).

In the study area, the aquifer is recharged from irrigation return flow and the irrigation canals of El Kalabia and Asfun and their tributaries (Figs. 2 and 3). There are some recharges from the several wadis dipping westward toward the River Nile, which are draining Red Sea Mountains. The groundwater discharge components in the study area include irrigations wells, discharge into the River Nile, and dewatering wells in the temple areas.

A piezometric map of the study area was drawn based on water level measurements from the twenty-nine wells (Fig. 3). This map shows that the groundwater flow in the study area is generally driven by topography with a downward gradient from east to west and southeast to northwest. The piezometric heads decrease gradually from 75 m in the eastern end of the area to less than 70 m near the Nile River, which plays as a main drain (Fig. 3). The former groundwater flow directions are dissected by northward flow, because of the northward dip direction of the strata of the Nile River aquifer. In the central part the El Kalabia canal plays a recharge source for groundwater, therefore it makes some modification of the regional groundwater flow toward the Nile River. The dewatering of archeological sites in Luxor City has resulted in a cone of depression, which modifies the regional direction of groundwater flow toward Luxor city, where the water level is as low as 69 m (Fig. 3).

2. MATERIALS AND METHODS

Detailed hydrogeological investigation was conducted, including water level measurements. Groundwater samples from twenty-nine wells that tap the alluvial aquifer and two samples from River Nile were collected and analyzed (Fig. 1). The water point collection and analysis followed the methods of Rice et al. (2012). Groundwater was sampled from each well after pumping until the flowing water was found to have a stable temperature (T) and electrical conductivity (EC). The T, pH and EC were measured at each site using a multi-parameter portable meter (HACH-HQ40d).

Most of the sampled wells are used for agricultural, domestic, and dewatering purposes. Location and elevation of each water point were recorded using a GPS (Fig. 1). The chemical analyses of the collected groundwater samples for major cations and major anions were carried out in the Environmental Research Laboratory, South Valley University. The chemical analyses for major cations (Ca^{2+}, Mg^{2+}, Na^{+}, K^{+}) were performed using an atomic absorption spectrophotometer (SpectrAA-55). A titration method was used for the measurement of the anions CO_3^{2-}, HCO_3^{-} and Cl^{-}. A spectrophotometer (DR/2400) was used for the analysis of SO_4^{2-} and NO_3^{-}.

Laboratory work was followed by data analyses using AquaChem and PHREEQC software to calculate saturation indices (SI) and other parameters. Geochemical modeling was carried out using PHREEQC (Parkhurst and Appelo, 1999) to calculate aqueous speciation and mineral saturation indices of reactive minerals in the system. The Spatial Analyst module (ArcGIS 10.3) was used to study spatiotemporal variation of the water table and groundwater quality in. A number of hydrochemical parameters were determined and analyzed to evaluate the chemistry of the groundwater (Table 1). The saturation indices were used to estimate mineral

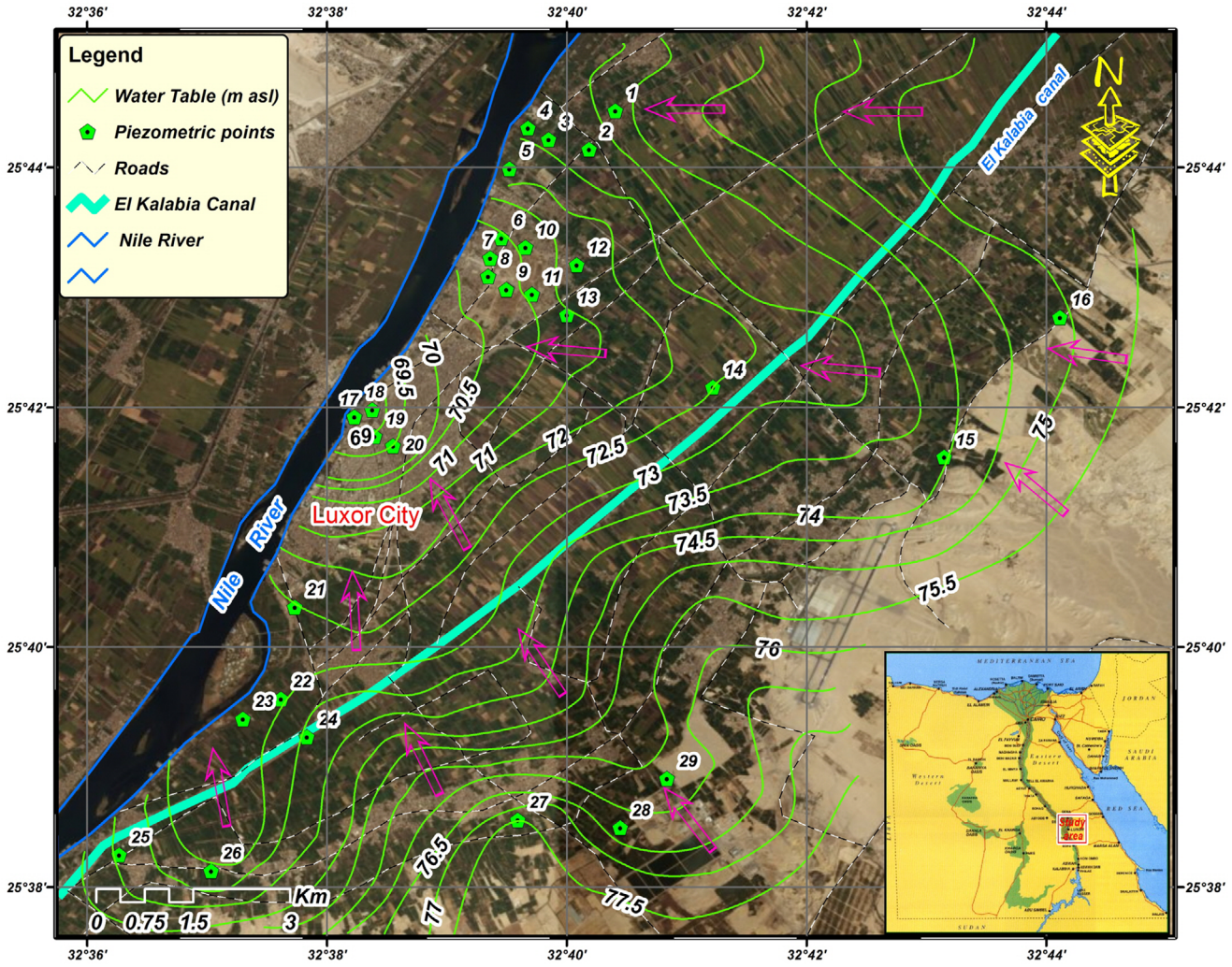

Fig. 3. Piezometric surface map based on its fitted semi-variogram.

reactivity in the groundwater; the reactive minerals of aquifer media can be predicted from groundwater without collecting samples of the solid phase for direct mineralogical analysis (Deutsch, 1997).

Chloro-alkaline indices (CAI-I and CAI-2), which were used to determine the ion-exchange processes in groundwater, were calculated in units of meq/l using the following formulae proposed by Schoeller (1956):

$$\text{CAI-1} = \text{Cl} - (\text{Na} + \text{K})/\text{Cl}, \quad (1)$$

$$\text{CAI-2} = \text{Cl} - (\text{Na} + \text{K})/\text{SO}_4 + \text{HCO}_3 + \text{CO}_3 + \text{NO}_3. \quad (2)$$

These indices indicate Base Exchange or non-exchange between sodium and potassium in water with calcium and magnesium in rocks according to this formula.

When groundwater flows, it interacts with the minerals of the aquifer, which is associated with geochemical dissolution and precipitation. The SI is a calculation of the interaction between groundwater and rock, and it was calculated for this study using the PHREEQC software. The SI of a particular mineral can be defined as:

$$\text{SI} = \log(K_{\text{IAP}}/K_{\text{sp}}), \quad (3)$$

where K_{IAP} is the ion activity product, and K_{sp} is the solubility product in respect of water sample temperature. A positive SI indicates supersaturation or precipitation of secondary minerals; however, precipitation is necessary to achieve equilibrium. A negative SI indicates undersaturation and that the dissolution of minerals is required to reach equilibrium. A SI of 0.5 indicates equilibrium conditions.

Descriptive statistics were calculated for the different variables of the groundwater samples; these statistics include the minima, maxima, averages, and standard deviations of the variables. The data were examined for normality using the nonparametric one-sample Kolmogorov-Smirnov test. Descriptive statistics and

https://doi.org/10.1007/s12303-018-0039-7

Table 1. Chemical analyses of major constituents of water points in the study area

ID	Well Depth (m)	DTW (m)	Temp (°C)	pH	EC	TDS	K^+	Na^+	Mg^{2+}	Ca^{2+}	Cl^-	NO_3^-	SO_4^{2-}	HCO_3^-	CO_3^{2-}	Water type	SI	SI	SI	SI	SI	SI
					µS/cm	mg/l	mg/l	mg/l	mg/l	mg/l	mg/l	mg/l	mg/l	mg/l	mg/l		Cal	Arg	Dol	Anh	Gyp	Hal
1	30	3.0	22.6	8.01	1062	349	2.50	62.38	21.14	16.70	32.50	0.30	160.00	53.80	5.90	$Na\text{-}SO_4$	−1.44	−1.59	−2.51	−2.23	−1.99	−7.25
2	30.5	3.0	23.7	8.51	917	578	23.00	95.00	28.97	27.66	48.53	1.00	190.00	163.80	1.80	$Na\text{-}SO_4$	−0.92	−1.07	−1.55	−2.01	−1.77	−6.91
3	30	0.5	22.9	8.12	1029	308	1.09	31.45	36.08	10.28	54.75	1.90	46.00	126.00	6.50	$Mg\text{-}HCO_3$	−1.34	−1.48	−1.83	−2.97	−2.73	−7.33
4	31	0.5	23.9	8.19	509	329	0.95	78.46	16.33	10.14	105.45	0.10	17.00	100.80	7.60	Na-Cl-	−1.38	−1.53	−2.27	−3.35	−3.12	−6.64
5	31	0.3	23.2	7.53	3004	1049	2.34	226.72	50.84	28.76	47.00	3.60	270.00	420.00	29.50	$Na\text{-}HCO_3$	−0.49	−0.64	−0.46	−1.96	−1.73	−6.58
6	30	5.0	23.8	8.16	2140	748	13.52	142.59	43.18	24.52	115.94	1.30	280.00	126.90	15.90	$Na\text{-}SO_4$	−0.98	−1.12	−1.43	−1.96	−1.72	−6.37
7	32	2.6	23.4	8.94	1218	467	16.24	136.00	9.10	5.77	158.35	1.90	30.00	109.20	21.20	Na-Cl	−1.47	−1.62	−2.48	−3.36	−3.12	−6.23
8	31.7	4.1	21.8	9.33	1425	586	81.00	113.68	27.15	3.03	124.29	1.20	78.00	157.50	39.75	Na-Cl	−1.60	−1.75	−1.97	−3.33	−3.09	−6.43
9	31	2.7	21.8	9.74	2100	716	14.35	177.66	34.30	26.67	129.26	1.60	156.00	175.80	63.60	Na-Cl	−0.57	−0.72	−0.75	−2.16	−1.93	−6.23
10	31.5	3.8	21.5	7.93	1857	631	8.91	105.76	33.33	36.56	55.93	0.40	270.00	120.00	10.60	$Na\text{-}SO_4$	−0.86	−1.00	−1.48	−1.78	−1.54	−6.81
11	31	6.0	21.0	8.05	1727	365	0.57	96.94	12.50	4.59	43.75	1.50	160.00	45.40	0.00	$Na\text{-}SO_4$	−2.21	−2.36	−3.73	−2.73	−2.50	−6.93
12	28	4.3	23.3	7.98	1518	423	4.13	84.24	20.84	20.26	16.00	0.20	210.00	67.80	10.20	$Na\text{-}SO_4$	−1.26	−1.41	−2.22	−2.07	−1.84	−7.44
13	28.2	4.0	21.4	7.79	741	244	1.15	48.00	15.00	10.00	56.50	0.20	42.00	70.80	1.80	Na-Cl	−1.60	−1.74	−2.74	−2.94	−2.70	−7.11
14	26.7	2.8	22.9	7.90	1110	710	0.97	208.00	20.00	3.24	164.75	1.20	110.00	201.60	21.20	Na-Cl	−1.67	−1.81	−2.23	−3.20	−2.96	−6.05
15	25.5	10.0	23.1	7.69	2739	1034	2.25	210.00	47.00	148.96	150.00	1.60	390.00	84.00	168.00	$Na\text{-}SO_4$	0.31	0.16	0.40	−1.21	−0.98	−6.13
16	25	16.5	22.1	7.74	5240	2061	2.63	551.29	28.80	126.35	285.00	2.60	980.00	84.00	39.00	$Na\text{-}SO_4$	−0.36	−0.51	−1.09	−0.99	−0.75	−5.45
17	25	7.3	23.3	7.53	1557	277	1.22	42.31	22.72	16.54	38.50	4.00	42.00	110.00	16.50	$Mg\text{-}HCO_3$	−1.04	−1.18	−1.66	−2.75	−2.52	−7.34
18	25.8	6.2	22.8	7.42	1534	457	0.65	39.87	37.92	44.19	65.56	14.20	61.00	193.20	16.50	$Mg\text{-}HCO_3$	−0.51	−0.65	−0.79	−2.28	−2.04	−7.15
19	27	5.7	21.7	8.72	656	220	13.00	46.00	9.31	8.32	27.12	1.90	40.00	74.00	15.90	$Na\text{-}HCO_3$	−1.45	−1.59	−2.56	−3.04	−2.80	−7.45
20	26	6.2	22.1	8.98	686	407	2.38	113.35	11.60	6.07	115.43	3.30	50.00	105.00	10.60	Na-Cl	−1.58	−1.73	−2.57	−3.13	−2.89	−6.45
21	26	4.0	23.3	7.87	3700	400	1.00	34.00	55.10	13.00	99.00	2.80	140.00	54.60	10.20	$Mg\text{-}SO_4$	−1.49	−1.63	−2.06	−2.46	−2.22	−7.05
22	27.6	3.6	23.4	8.17	461	187	1.11	26.00	15.00	6.07	10.53	2.40	22.00	103.48	2.93	$Mg\text{-}HCO_3$	−1.63	−1.78	−2.58	−3.40	−3.16	−8.08
23	27	4.7	23.9	8.08	995	300	1.66	53.62	20.65	4.97	31.50	0.20	50.00	137.50	6.50	$Na\text{-}HCO_3$	−1.59	−1.74	−2.28	−3.19	−2.95	−7.32
24	25.5	4.5	23.8	8.18	768	380	2.44	91.55	19.30	6.66	60.50	0.20	32.00	167.70	21.20	$Na\text{-}HCO_3$	−1.28	−1.43	−1.85	−3.26	−3.03	−6.81
25	24.4	2.8	22.9	8.02	1100	278	2.20	61.65	16.82	8.00	75.50	2.20	49.00	63.00	10.20	Na-Cl	−1.59	−1.74	−2.58	−2.99	−2.75	−6.88
26	25	4.9	24.0	7.96	1210	254	1.62	69.00	7.00	4.00	32.00	8.80	38.00	94.00	17.00	$Na\text{-}HCO_3$	−1.68	−1.83	−2.84	−3.36	−3.12	−7.20
27	25	9.2	27.0	7.30	1190	812	10.22	141.00	24.00	131.00	121.00	56.20	120.00	278.00	5.16	$Ca\text{-}HCO_3$	−0.04	−0.19	−0.54	−1.63	−1.39	−6.36
28	25.6	10.3	25.0	7.60	1073	685	6.13	132.00	23.00	114.00	51.00	54.30	140.00	281.00	2.43	$Na\text{-}HCO_3$	−0.11	−0.26	−0.63	−1.60	−1.37	−6.76
29	24	8.9	26.0	7.80	1066	693	6.38	131.00	24.00	113.00	54.00	60.10	145.00	277.00	4.35	$Na\text{-}HCO_3$	−0.11	−0.26	−0.61	−1.59	−1.36	−6.74
30 (N.R.1)	–	–	26.0	8.1	461	294	3.70	21.82	9.49	25.44	10.45	0.80	17.57	194	1.9	$Ca\text{-}HCO_3$	−0.79	−0.92	−1.70	−2.90	−2.67	−8.19
31 (N.R.2)	–	–	26.5	8.2	431	276	3.17	19.16	8.30	22.56	8.19	0.70	10.70	191	1.5	$Ca\text{-}HCO_3$	−0.83	−0.98	−1.81	−3.15	−2.92	−8.35
Min	24	0.3	21.0	7.30	461	187	1	26	7	3	11	0.1	17	45	0	–	−2.21	−2.36	−3.73	−3.40	−3.16	−8.08
Max	32	16.5	27.0	9.74	5240	2061	81	551	55	149	285	60	980	420	168	–	0.31	0.16	0.40	−0.99	−0.75	−5.45
Mean	28	5.1	23.2	8.11	1529	550	8	116	25	34	82	8	149	140	20	–	−1.10	−1.25	−1.79	−2.52	−2.28	−6.81
SD	2.6	3.4	1.3	0.56	1036	373	15	101	13	45	59	17	186	86	32		0.62	0.62	0.92	0.73	0.73	0.54

DTW = Depth To Water, N.R.1 = Nile River No. 1, N.R.2 = Nile River No. 2, Min = Minimum, Max = Maximum, SD = Standard deviation, SI = Saturation index, Cal = Calcite, Arg = Aragonite, Dol = Dolomite, Anh = Anhydrite, Gyp = Gypsum, Hal = Halite.

Pearson correlation coefficients were determined to inspect the hydrochemical evolution of the variables (Tables 1 and 2). The spatial distribution of salinity was determined using the fitted universal kriging semi-variogram model. Semi-variograms quantify spatial continuity and are governed by the vector h, with its origin at x_i, that separate a given pair of measurements. A semi-variogram can be assessed using the experimental semi-variogram $\gamma(h)$ as follows:

$$\gamma(h) = \frac{1}{2n(h)} \sum_{(i,j):h_{ij}=h} (x_i - x_j)^2, \quad (4)$$

where $\gamma(h)$ is the semi-variance for the distance class h, $n(h)$ is the total number of pairs of values at distance h, and h_{ij} is the distance between locations i and j.

Spatial variability is well-defined by computing experimental variograms because different kriging methods are applied (Ahmadi and Sedghamiz, 2007; Babiker et al., 2007). For comparing the observed and predicted variable values, least error models are applied. The cross-validation test is used to determine the reliability of the approved models.

The original dataset was standardized using standards given by Davis (2002), which allowed the measurements analysis of various concentrations and parameters of different units. Both factor and cluster analyses were made to recognize the factors

that were significant to water geochemical processes and categorized groundwater areas (Jiang et al., 2009; Andrade and Stigter, 2011).

Cluster analysis was applied to investigate and identify groundwater systems by discretization of the area of study into different zones, which might be significant in geological, hydrological, and environmental contexts. Variance was calculated to ensure precision of the distances between clusters and to decrease the sum of squares of any two clusters that could be molded. Factor scores for each sampling locations were used as variables; samples with related factor scores were grouped into the similar cluster. To avoid misclassification caused by dissimilar orders of magnitude and variances of the variables, the variances are standardized to the equivalent Z scores, which were calculated as follows:

$$Z_{ij} = \frac{x_i - \mu_i}{\sigma_i}, \quad (5)$$

where X_i is the value for variable $_i$, and μ_i and σ_i are the mean and standard deviation of the same variable. The outcomes of cluster analysis are justified based on realistic hydrochemical, hydrological, and environmental patterns representing field conditions.

Factor analysis is an effective application for the expression of factors that affect groundwater quality and hydrochemical processes (Liu et al., 2003; El Alfy et al., 2017). The STATISTICA-10 software package (StatSoft Inc., 2004–2011) was used with 14 hydrochemical variables to perform R-mode factor analysis using orthogonal varimax rotation.

3. RESULTS AND DISCUSSION

The physicochemical and ion compositions of the groundwater samples were statistically analyzed. The maximum, minimum, average and standard deviation are considered (Table 1). The dominant cation in groundwater is Na^+, followed closely by Mg^{2+}. Among the anions, Cl^- has the highest concentration, followed by SO_4^{2-}. Concentrations of ions in most of the groundwater samples followed the order $Na^+ > Mg^{2+} > Ca^{2+} > K^+$ for cations, and $Cl^- > SO_4^{2-} > HCO_3^- > NO_3^-$ for anions. In certain samples, concentrations of Ca^{2+} exceed Mg^{2+} and concentrations of HCO_3^- exceed SO_4^{2-}.

The pH values of the groundwater samples vary between 7.30 and 9.74, with an average of 8.11; which reflects a slightly alkaline nature of the groundwater in this region, and specifies that dissolved carbonates are mainly HCO_3^-. The TDS values vary between 187 mg/l and 2,061 mg/l with an average value of 550 mg/l. More than 88.5% of the samples are freshwater (< 1,000 mg/l), while the rest of the samples are brackish. The TDS values are strongly correlated with Na^+, Cl^- and SO_4^{2-} concentrations, which indicates that these ions are major controlling variables of groundwater salinity. Salinity decreases from the eastern part of the aquifer toward the River Nile in the west following the direction of groundwater flow (Fig. 4). In the central part of the study area, the groundwater salinity distribution is influenced by infiltration of the fresh water of El Kalabia canal. The infiltrated fresh water (< 300 mg/l) mixes with the down gradient flow brackish groundwater (1200–2000 mg/l) resulting in moderate phase of groundwater salinity (600–1000 mg/l) (Fig. 4). In the western part of the study area, there is a narrow belt parallel to the Nile River has low salinity values (200–400 mg/l), which shows clearly the influence of recharge with fresh River Nile water (< 200 mg/l).

NO_3^- concentrations vary between < 1 and 60 mg/l, with an average value of 8 mg/l (Table 1). The spatial distribution of NO_3^- in the groundwater shows low concentration values to the east represent background concentration (Fig. 5). The higher concentration values are recorded near the wastewater treatment plant (southeastern part). It reflects the human impact influencing groundwater quality in this area, where unsewered urban areas have long-term influence. The treated water is used in irrigation of 1700 feddans of timber tree forest (mahogany, jatropha, mulberry, and physic nut) with modified flood and drip irrigation systems. The excess of irrigation return flow water reaches the groundwater since the aquifer has low buffer capacity and the water table is shallow.

Piper (1944) diagram is extensively used to investigate the groundwater geochemical evolution (Fig. 6), to identify water origins and hydrogeochemical facies (Freeze and Cherry, 1979; Chidambaram et al., 2008; Karmegam et al., 2010; Abdalla and Scheytt, 2012). In Figure 6, the results of the chemical analyses are plotted in a Piper diagram, where this diagram can better represent noisy data (Domenico and Schwartz, 1998). The Piper diagram shows that 54% of groundwater samples are of the NaCl and $NaSO_4$ water types and 11.5% are of the $CaHCO_3$ type, whereas 27% fall into no-dominant or mixed class types (five samples are a mixed Ca,Na-HCO_3 type and two samples are a mixed Ca,Mg-Cl type). Piper diagram classification shows that the majority of samples belong to the NaCl and $NaSO_4$ water types, which confirms that the water chemistry is influenced by secondary processes such as groundwater mixing with irrigation return flow and sewage leakage. Higher Cl and SO_4 concentrations can indicate the influence of mixing between groundwater and wastewater as well as the applications of fertilizers (KCl and K_2SO_4) in the study area. A Durov plot has been used to help interpret the dissolution and mixing processes of ions and identify the prevailing hydrochemical processes (Fig. 6). The plot for the collected samples shows that 52% of samples are dominated by the anion SO_4^{2-} and the cation Na^+. This finding

https://doi.org/10.1007/s12303-018-0039-7

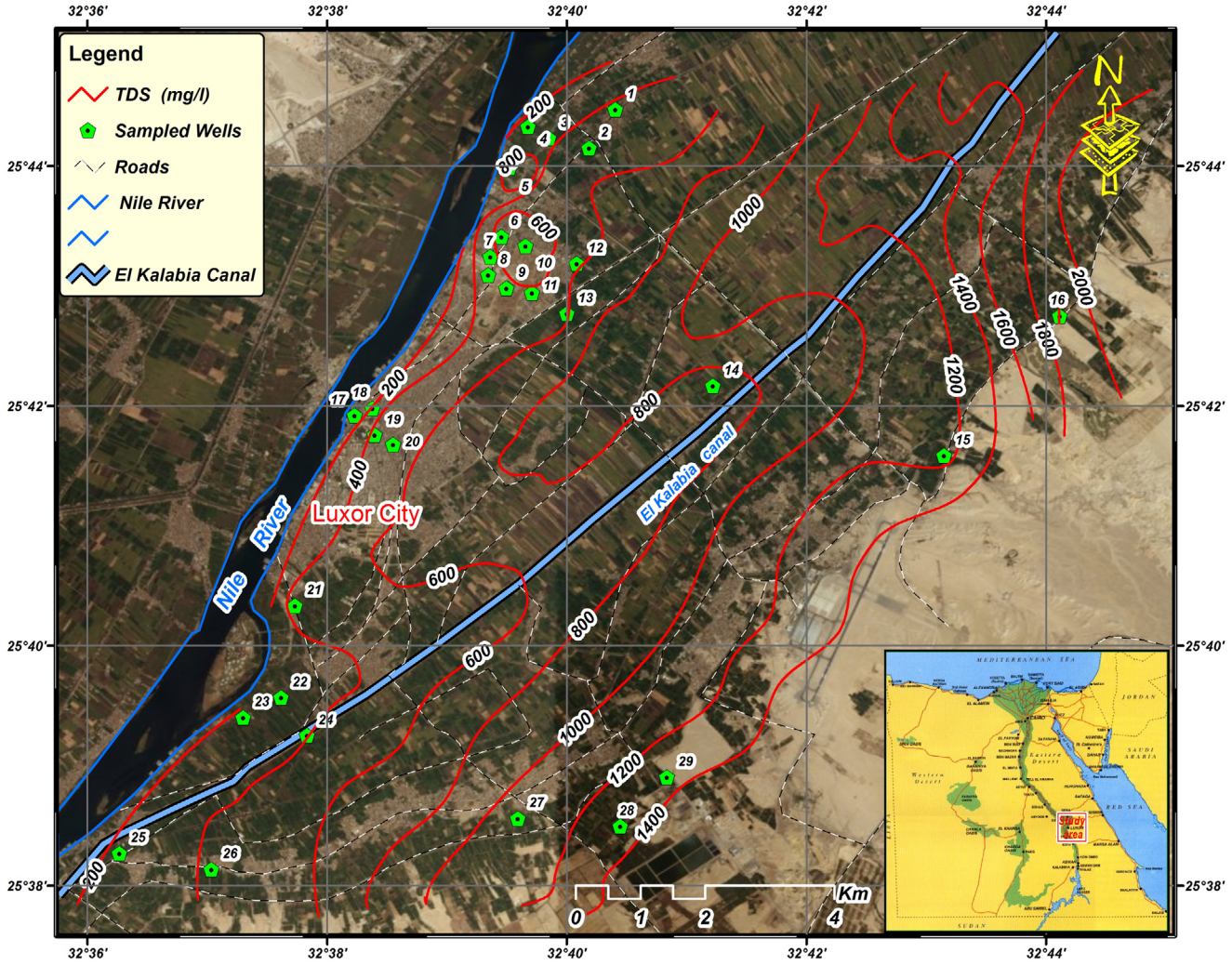

Fig. 4. Spatial distribution of TDS in the Luxor area based on its fitted semi-variogram.

indicates a reverse ion-exchange process. 34% of the water samples are found to have water types with no dominant anion or cation, which indicates the mixing of waters with different origins. 14% of the water samples plot represents the $MgHCO_3$ and $NaHCO_3$ facies. Therefore, these samples represent groundwater influenced by recharge processes from the River Nile and from irrigation return flow. The land-use/land-cover of the study area shows that, the source of irrigation water is the low salinity water (285 mg/l) of the River Nile and its connected tributaries and canals (Table 1), the excess of irrigation water infiltrates reaching the brackish groundwater (1400–2000 mg/l) flowing downstream from the eastern parts of the study area (Fig. 4). The salinity contour map shows this mixing process between the two water types giving a transition zone of slightly brackish water (600–1200 mg/l) below the cultivated areas. The elevated nitrate concentrations in the groundwater were directly related to the timing of land-surface application of treated water and leakage of sewage water (Fig. 5).

To confirm the exchange between sodium and/or potassium with calcium and/or magnesium in the aquifer, the chloro-alkaline indices (CAI-I and CAI-2) of the groundwater samples were calculated. The calculated values of CAI-2 and CAI-1 (Fig. 7) show that 78.3% of the CAI-2 values and 48% of the CAI-1 values are positive, which reflects the strong influence of reverse ion-exchange processes.

The saturation indices (SI) of the major mineral phases in the analyzed water points, including the calcite, aragonite, dolomite, anhydrite, gypsum and halite phases, were also considered (Table 1). The carbonate SIs indicate undersaturation with respect to all of the above minerals. The SI values for all examined samples indicate high undersaturation with respect to halite. Undersaturation of these minerals causes dissolution of carbonate and sulfate minerals, which produces high Ca^{2+} and Mg^{2+} concentrations in groundwater.

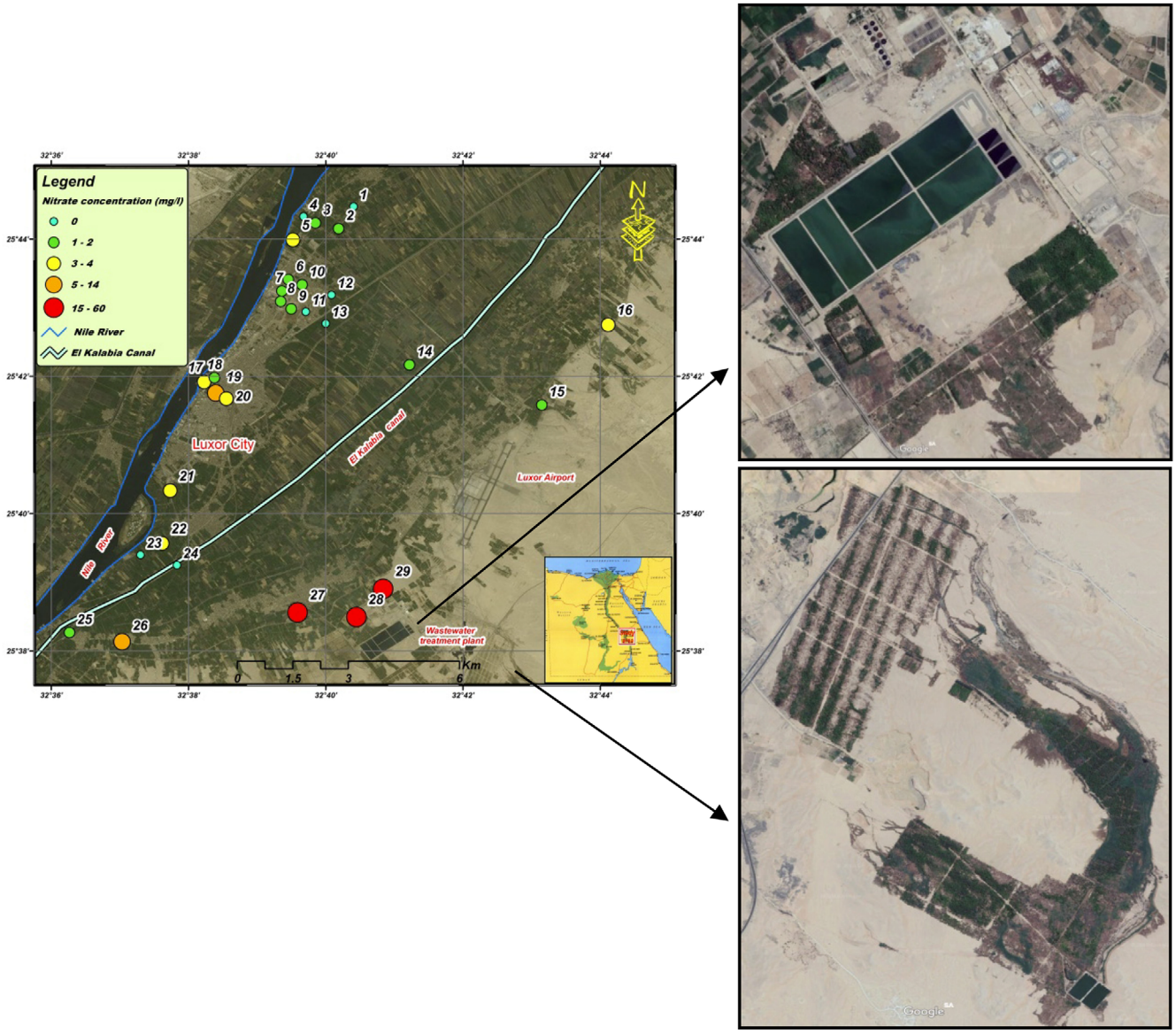

Fig. 5. Spatial distribution of nitrate concentration in the study area, showing the wastewater treatment plant (the upper right photo) and the timber tree forest (the lower right photo).

The correlation coefficient matrix between the measured hydrochemical variables was prepared using Pearson correlation (Table 2). There are strong correlations between EC and TDS, Na^+, Mg^{2+}, Cl^-, SO_4^{2-}, Ca^{2+}, and NO_3^-, which is because EC and TDS are measures of the total dissolved solids in groundwater.

Strong correlations are also detected between the TDS and Na^+, SO_4^{2-}, Cl^-, Mg^{2+}, CO_3^-, and Ca^{2+} (Table 2). These findings demonstrate that the key factors that influence groundwater salinity are the levels of dissolution of aquifer minerals such as halite, gypsum, anhydrite, aragonite and calcite, which is consistent with the undersaturation phases of these minerals (Table 1). The cations Ca^{2+} and Mg^{2+} have strong correlation coefficients with SO_4^{2-}, which represents the presence an abundant source of Ca^{2+} and Mg^{2+}; this source may be the dissolution of the carbonate and dolomite minerals. The strong and moderate correlations between Na^+ and Ca^{2+} or SO_4^{2-} reflect the influence of ion-exchange on groundwater hydrochemistry. This strong impact is confirmed by the Piper and Durov diagram (Fig. 6).

Cluster analysis was performed, and the z-standardized input data matrix for the twenty-nine groundwater samples with 14 hydrochemical variables is represented by Q-mode dendrograms (Fig. 8). To calculate the variation among the clusters and to review the appearances of samples in dissimilar clusters, the average values of measurements from chemical analyses and the physicochemical parameters are obtained (Table 3). Cluster analysis is interpreted at a similarity linkage distance of 1,400,

https://doi.org/10.1007/s12303-018-0039-7

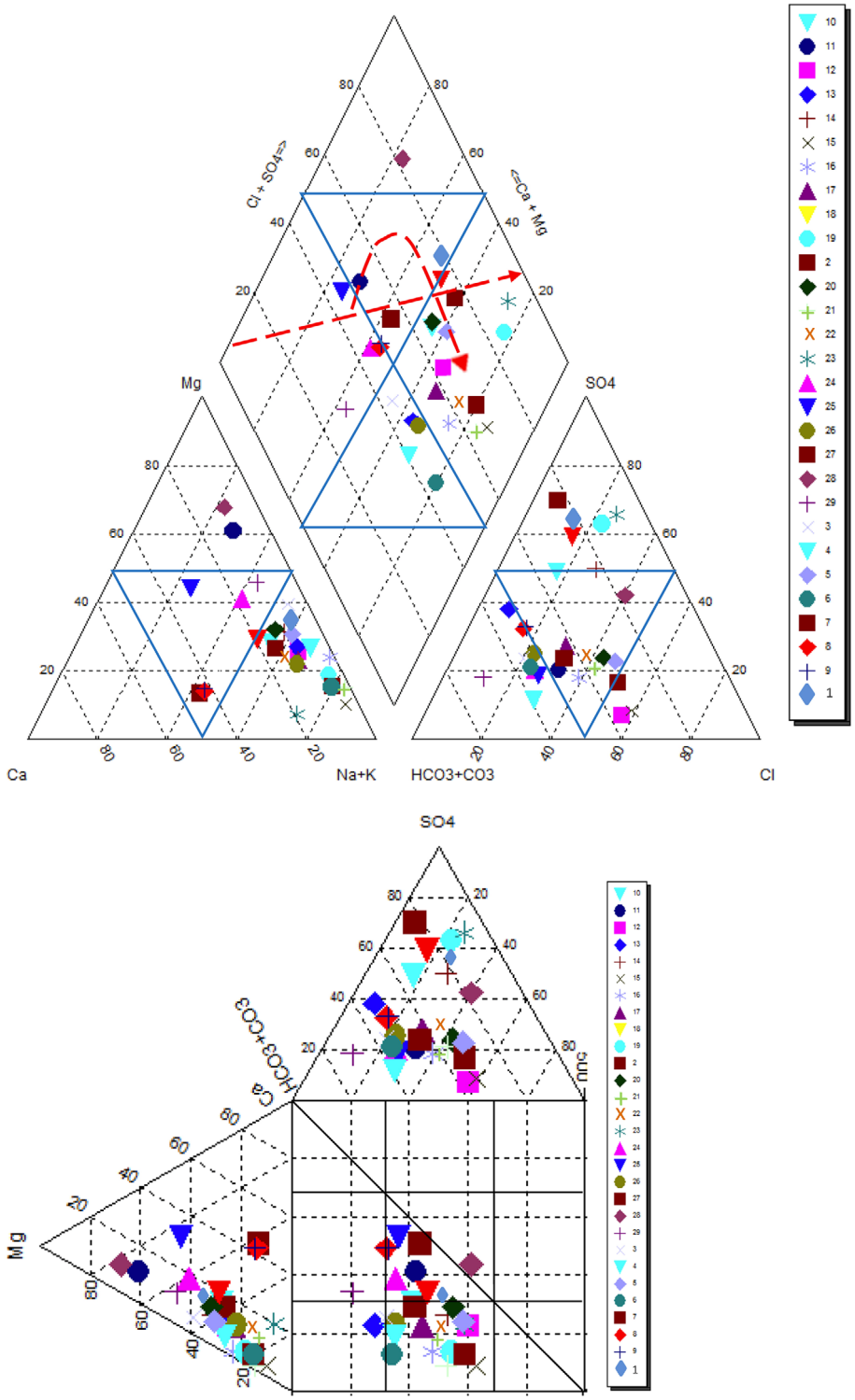

Fig. 6. Piper diagram and Durov diagram of the groundwater samples.

based on which all groundwater samples are categorized into four significant clusters (Fig. 8). These clusters are verified according to the zonation of the water table, land use, and hydrochemical processes. The water table is categorized into deep, moderate, and shallow zones, whereas land-use is classified into rural, agricultural, and urban areas. Hydrochemical processes are grouped into recharge, mixing with water from the River Nile, and irrigation return flow. Figure 9 displays the spatial distribution of the four distinct groundwater clusters of the study area. The first cluster starts near the wastewater treatment

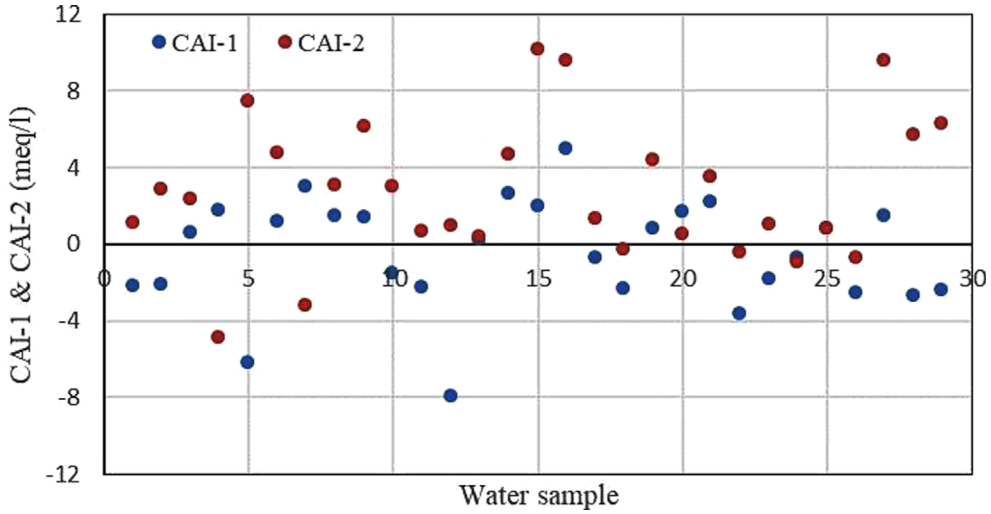

Fig. 7. Plots of CAI-I and CAI-2 values for groundwater samples from the study area.

Table 2. Correlation Coefficients among different water variables

	pH	EC	TDS	K^+	Na^+	Mg^{2+}	Ca^{2+}	Cl^-	NO_3^-	SO_4^{2-}	HCO_3^-	CO_3^{2-}
pH	1.00	–0.49	–0.11	0.49	0.07	–0.39	–0.44	0.07	–0.30	–0.34	0.11	–0.08
EC		1.00	0.69	0.12	0.48	0.66	0.50	0.37	0.33	0.73	0.04	0.50
TDS			1.00	0.40	0.84	0.61	0.49	0.66	0.00	0.76	0.43	0.60
K^+				1.00	0.46	0.08	0.18	0.16	–0.19	0.29	0.18	0.35
Na^+					1.00	0.17	0.18	0.62	–0.11	0.58	0.29	0.61
Mg^{2+}						1.00	0.71	0.25	0.10	0.67	0.34	0.26
Ca^{2+}							1.00	0.12	0.11	0.61	0.07	0.17
Cl^-								1.00	0.04	0.23	0.24	0.57
NO_3^-									1.00	–0.03	0.05	0.32
SO_4^{2-}										1.00	0.02	0.20
HCO_3^-											1.00	0.44
CO_3^{2-}												1.00

plant in the eastern part and extends as a plume toward the Luxor urban area, and it reflects the human impact on groundwater quality. Where high pH and high concentrations of potassium and nitrate were recoded (Table 3, Fig. 10), contamination of groundwater with sewage wastewater is indicated. The second cluster is situated in the eastern part and stretches westward in a narrow tongue north of Luxor city, which may indicate an east-west paleochannel that drains into the River Nile. This cluster reflects the groundwater that is recharged from the eastern Red Sea Mountains and flows for long distances; samples of this cluster have the highest recorded TDS and concentrations of Na^+, Cl^-, and SO_4^{2-}, and the smallest negative saturation indices of the dominant mineral phases (Table 3, Fig. 10). The third cluster is found to the north and south of the first cluster, and is largely bounded to the east by the El Kalabia canal. This cluster represents cultivated areas, and shows the mixing between groundwater and irrigation return flow. Groundwater is very shallow in this area (i.e., the depth to the groundwater is < 3 m), and the concentration of HCO_3^- has the highest value of the four clusters (Table 3, Fig. 10). The fourth cluster is bounded by the River Nile, representing groundwater recharge by the fresh water of the River Nile; it has the lowest TDS and major ion concentrations, and the highest negative saturation indices for the various mineral phases (Table 3, Fig. 10).

Factor analysis identified four significant factors with eigenvalues > 1, using orthogonal varimax rotation. Table 4 shows these factors, rotated factor loadings, eigenvalues, and the proportion of variance they explain. These factors account for a cumulative total variance of 73.64%, with a minimum eigenvalue of 1.04, and cumulative eigenvalues of 11.05 (Table 4, Fig. 11).

The first factor explains 39.95% of the total variance and 5.99 of the eigenvalue; it shows strong positive loadings with EC, TDS, SO_4^{2-}, Na^+, Ca^{2+}, EC, Cl^-, depth to water (DTW) and CO_3^{2-}, and relatively weak loading with Mg^{2+} (Table 4, Fig. 11).

https://doi.org/10.1007/s12303-018-0039-7

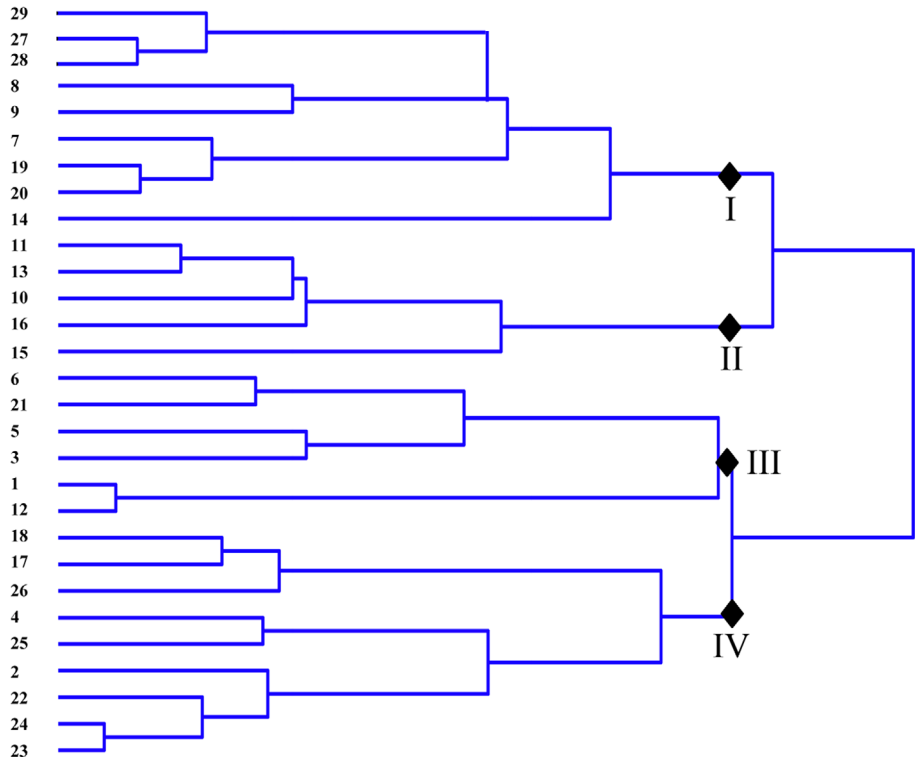

Fig. 8. Dendrogram of the distinct groundwater clusters of the study area (complete linkage, 1 – Pearson r).

Table 3. Average values of the four clusters variables

	DTW	Temp °C	pH	TDS mg/l	K mg/l	Na mg/l	Mg mg/l	Ca mg/l	Cl mg/l	NO_3 mg/l	SO_4 mg/l	HCO_3 mg/l	CO_3 mg/l	SI Cal	SI Arg	SI Dol	SI Anh	SI Gyp	SI Hal
Cluster I	4.26	22.2	9.1	479.2	25	117	18	10	111	2.0	71	124	30.4	−0.9	−1.0	−1.5	−1.5	−2.2	−6.6
Cluster II	8.06	21.8	7.8	867.0	3.2	202	27	65	118	1.4	368	81	44	−1.0	−1.1	−1.7	−1.1	−1.7	−6.5
Cluster III	2.85	23.2	7.9	546.2	4.2	97	38	19	61	1.7	184	142	13.2	−1.2	−1.3	−1.8	−1.3	−2.0	−7.0
Cluster IV	4.17	23.5	8.0	337.8	3.9	62	21	14	52	3.6	56	126	11.3	−1.3	−1.4	−2.1	−1.4	−2.7	−7.1

This factor may be attributed to the increasing groundwater salinity that results from dissolution of carbonate minerals (calcite, aragonite, and to a lesser degree dolomite) and evaporite minerals (halite, gypsum, and anhydrite), which are frequently encountered in the aquifer media. This factor is strongly correlated with the SIs of the tested minerals (Table 1). Generally, the dissolution processes occur at relatively greater depths; this can be confirmed by the high loading of DTW (0.79). The second factor accounts for 15.39% of the total variance and 2.31 of the eigenvalue. This factor represents higher loadings for pH and K^+ (Table 4, Fig. 11). This factor may reflect the leaching of potassium and iron ions from feldspar minerals in the aquifer as groundwater migrates downstream.

The third factor accounts for 11.34% of the total variance and 1.70 of the eigenvalue; it includes higher loadings for HCO_3^- and Mg^{2+}, and low loading for DTW (Table 4, Fig. 11). This factor may reflect the dissolution of dolomite and the resulting release of Mg^{2+} with relatively deep groundwater percolation.

The fourth factor accounts for 6.96% of the total variance and 1.04 of the eigenvalue; it includes high loading for NO_3^- and low loadings for temperature and HCO_3^- (Table 4, Fig. 11). This factor reflects groundwater contamination with wastewater associated with a weak drainage system.

4. CONCLUSIONS

For this research, hydrochemical investigations including chemical analyses, multivariate statistics, and geostatistics were conducted to define the origins of groundwater and the factors that control groundwater geochemistry. Two samples from the El Kalabia canal which originates in the Nile River and twenty-nine groundwater samples were collected. For each sample, fourteen physiochemical variables were examined. Spatial changes

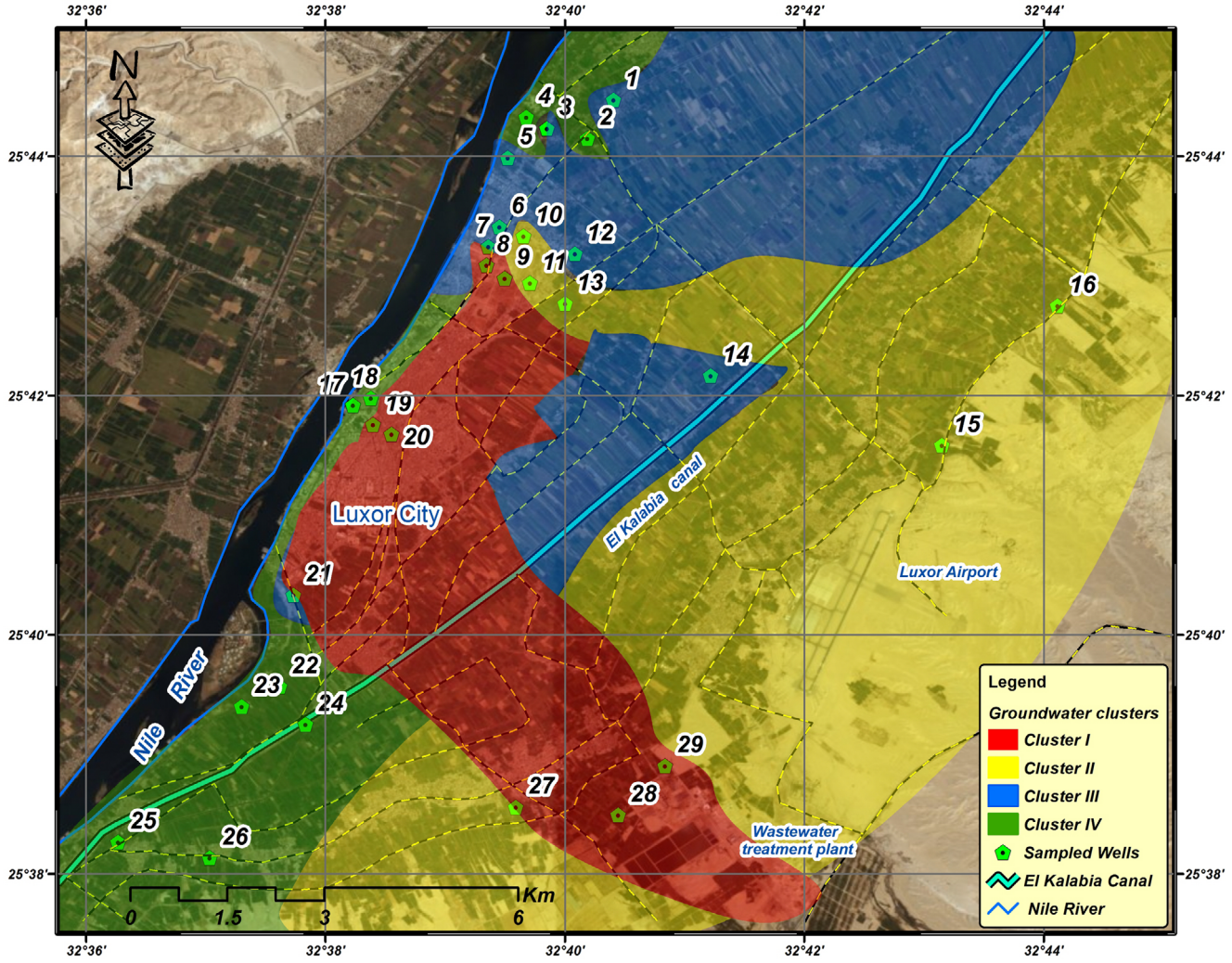

Fig. 9. Spatial distribution of the four groundwater clusters of the study area.

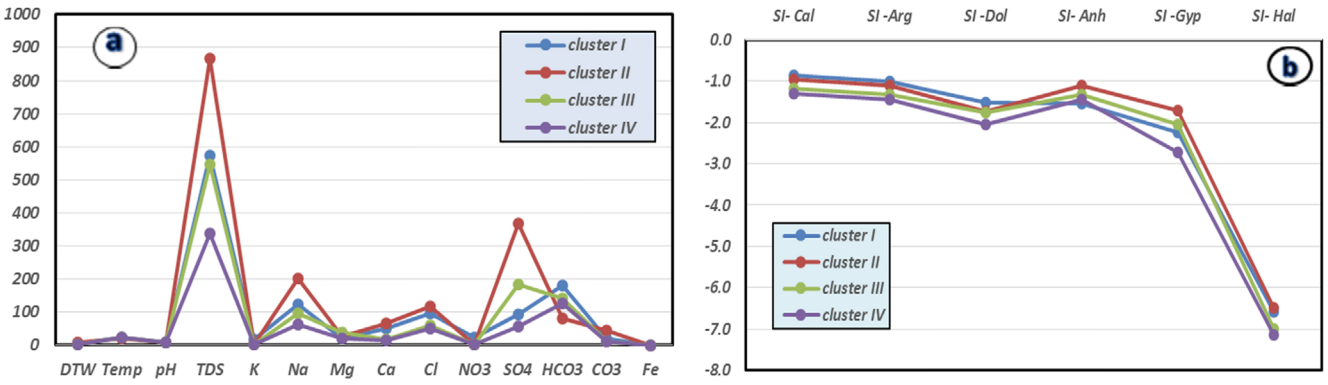

Fig. 10. Average variable values of the four clusters for (a) major ions, and (b) saturation indices.

in TDS and nitrate concentration that affect groundwater quality were mapped using fitted variograms; they show that the aquifer has high vulnerability to contamination. Anthropogenic activities near the wastewater treatment plant and around the residential areas of Luxor are recognized as additional processes that influence the hydrogeochemical properties of the groundwater. Piper diagram classification illustrates that the majority of samples belong to the NaCl and $NaSO_4$ water types, which

https://doi.org/10.1007/s12303-018-0039-7

Table 4. Factor analysis loadings and eigenvalues of the 29 samples and 14 variables

	Factor 1	Factor 2	Factor 3	Factor 4
DTW	0.79	–0.18	–0.41	0.10
Temp	–0.21	–0.28	0.31	0.39
pH	–0.13	0.90	–0.10	–0.11
EC	0.85	–0.17	0.23	–0.04
TDS	0.95	0.05	0.21	0.01
K^+	0.02	0.76	0.20	–0.17
Na^+	0.92	0.13	0.05	0.03
Mg^{2+}	0.39	–0.21	0.74	–0.13
Ca^{2+}	0.87	–0.24	0.06	–0.02
Cl^-	0.80	0.30	–0.03	0.05
NO_3^-	0.02	–0.26	0.12	0.78
SO_4^{2-}	0.94	–0.12	0.00	–0.11
HCO_3^-	0.02	0.14	0.82	0.28
CO_3^{2-}	0.59	0.08	0.20	–0.03
Explained variance	5.90	2.11	1.93	1.10
Proportion of factors' variance in the total variance	0.39	0.14	0.13	0.07
Eigenvalue	5.99	2.31	1.70	1.04
Total variance	39.95	15.39	11.34	6.96
Cumulative eigenvalue	5.99	8.30	10.00	11.05
Cumulative total variance (%)	39.95	55.34	66.68	73.64

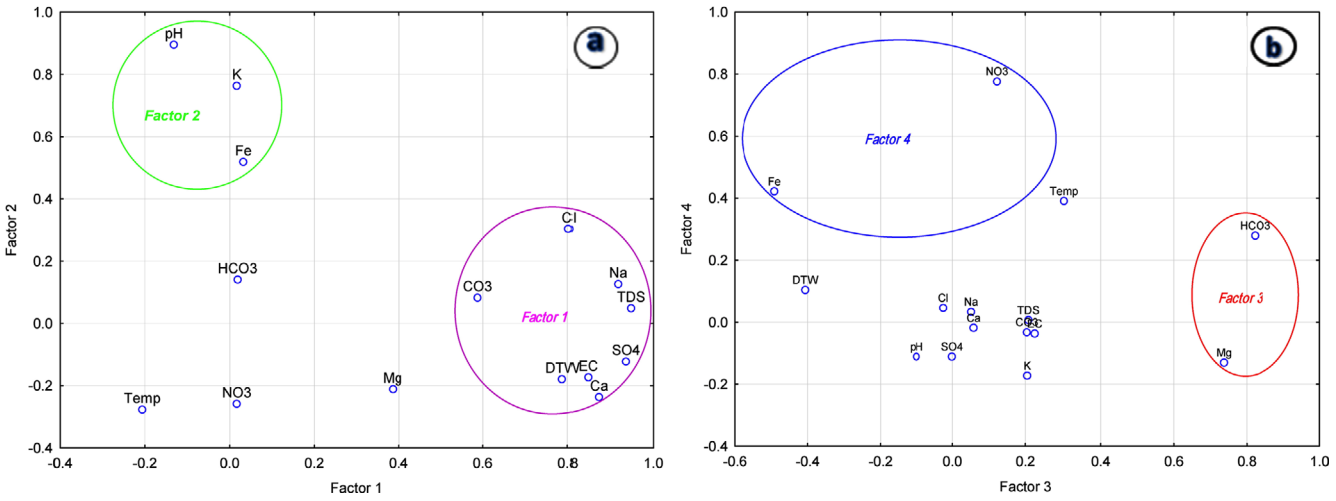

Fig. 11. Factor loadings for (a) Factor 1 vs. Factor 2, (b) Factor 3 vs. Factor 4.

confirms that the water chemistry is influenced by secondary processes such as groundwater mixing with irrigation return flow and sewage leakage. The Durov diagram and chloro-alkaline indices indicate that most samples are dominated by reverse ion-exchange processes, whereas fewer samples represent the mixing of waters of different origins. The SI values indicate that most of the groundwater samples are undersaturated with respect to the calcite, aragonite, dolomite, anhydrite, gypsum, and halite mineral phases. The main process determining the overall geochemical evolution of the groundwater system is water-rock interactions along the flow-path, such as carbonate dissolution and cation exchange processes. Correlation coefficients are consistent with the saturation indices of the aquifer minerals, and can be used to identify the different processes that contribute to groundwater hydrochemistry, dissolution of aquifer minerals, and ion exchange. Cluster analysis shows that there are four significant clusters of samples, which indicates that there are four distinct groundwater zones where the original groundwater may be more affected by mixing with irrigation return flow, by fresh water from the River Nile and irrigation canals, or by

contamination with sewage wastewater. Four factors were identified that describe > 73% of the total data variance. The factors mutually interfere, and they reveal which chemical properties of the groundwater are caused by rock-water interactions, mixing, or anthropogenic influences. The first three factors indicate the dissolution of various minerals, whereas the fourth factor indicates anthropogenic contamination with nitrate. It is expected that this anthropogenic factor may accelerate deterioration of the groundwater. These findings may be used for the better management of water resources on a regional scale and may be applicable to many areas with similar conditions.

ACKNOWLEDGMENTS

The authors wish to express their gratitude to the editor and the reviewers. The authors would like to extend their sincere appreciation to the Deanship of Scientific Research at King Saud University for funding through Research Group RG-1437-012.

REFERENCES

Abd El-Bassier, M., 1997, Hydrogeological and hydrochemical studies of the Quaternary aquifer in Qena Governorate. M.Sc. Thesis, Faculty of Science, Assiut University, Assiut, 120 p.

Abd El-Monim, A., 1986, Hydrogeology of the Nile Basin in Sohage Province, M.Sc. Thesis, Sohage Faculty of Science, Assuit University, Assiut, 165 p.

Abdalla, F. and Scheytt, T., 2012, Hydrochemistry of surface water and groundwater from a fractured carbonate aquifer in the Helwan area, Egypt. Journal of Earth System Science, 121, 109–124.

Abdalla, F., Ahmed, A., and Omr, A., 2009, Degradation of groundwater quality of Quaternary aquifer at Qena, Egypt. Journal of Environmental Studies, 1, 19–32.

Ahmadi, H. and Sedghamiz, A., 2007, Geostatistical analysis of spatial and temporal variations of groundwater level. Environmental Monitoring and Assessment, 129, 277–294.

Andrade, A. and Stigter, T., 2011, Hydrogeochemical controls on shallow alluvial groundwater under agricultural land: case study in central Portugal. Environmental Earth Sciences, 63, 809–825.

Attia, F., 1985, Management of water system in Upper Egypt. Ph.D. Thesis, Faculty of Engineering, Cairo University, Cairo, 356 p.

Babiker, I., Mohamed, A., and Hiyama, T., 2007, Assessing groundwater quality using GIS. Water Resource Management, 21, 699–715.

Chidambaram, S., Ramanathan, A., Prasanna, M., Lognathan, D., Badrinarayanan, T., Srinivasamoorthy, K., and Anandhan, P., 2008, Study on the impact of tsunami on shallow groundwater from Portnova to Pumpuhar, using geoelectrical technique-south east coast of India. Indian journal of marine sciences, 37, 121–131.

Davis, J., 2002, Statistics and Data Analysis in Geology. John Wiley & Sons, New York, 656 p.

Deutsch, W., 1997, Groundwater Geochemistry: Fundamentals and Application to Contamination. CRC Press, Boca Raton, 232 p.

Domenico, P. and Schwartz, F., 1998, Physical and chemical hydrogeology (2nd edition). John Wiley & Sons Inc., New York, 824 p.

EGSM (Egyptian Geological Survey and Mining Authorities), 1981, The geological map of Egypt. Scale 1: 2000000. Ministry of industry and mineral resources, 1 p.

El Alfy, M., 2013, Hydrochemical modeling and assessment of groundwater contamination in northwest Sinai, Egypt. Water Environment Research, 85, 211–223.

El Alfy, M., Lashin, A., Al-Arifi, N., and Al-Bassam, A., 2015, Groundwater characteristics and pollution assessment using integrated hydrochemical investigations GIS and multivariate geostatistical techniques in arid areas. Water Resources Management, 29, 5593–5612.

El Alfy, M., Lashin, A., Abdalla, F., and Al-Bassam, A., 2017, Assessing the hydrogeochemical processes affecting groundwater pollution in arid areas using an integration of geochemical equilibrium and multivariate statistical techniques. Environmental Pollution, 229, 760–770.

Ezz El Deen, H., El Sayed, A., and Barseem, M., 2013, The impact of subsurface geological structure on the groundwater occurrence using geophysical techniques in wadi El Kallabiyyah and wadi As Sabil, East Esna, Eastern Desert, Egypt. Arabian Journal of Geoscience, 7, 2151–2163.

Freeze, A. and Cherry, J., 1979, Groundwater. Prentice-Hall Inc., Englewood Cliffs, 603 p.

Jiang, Y., Wu, Y., Groves, C., Yuan, D., and Kambesis, P., 2009, Natural and anthropogenic factors affecting the groundwater quality in the Nandong karst underground river system in Yunan, China. Journal of Contaminant Hydrology, 109, 49–61.

Karmegam, U., Chidambaram, S., Sasidhar, P., Manivannan, R., Manikandan, S., and Anandhan, P., 2010, Geochemical characterization of groundwaters of shallow coastal aquifer in and around Kalpakkam, South India. Research Journal of Environmental and Earth Sciences, 2, 170– 177.

Lawrence, F. and Upchurch, S., 1982, Identification of recharge areas using geochemical factor analysis. Ground Water, 20, 680–687.

Liu, C., Lin, K., and Kuo, Y., 2003, Application of factor analysis in the assessment of ground water quality in a blackfoot disease area in Taiwan. Science of the Total Environment, 313, 77–89.

Moubark, K., 2013, Environmental impact of groundwater rising level on some archaeological sites in Upper Egypt. Ph.D. Thesis, South Valley University, Qena, 211 p.

Omran, A., Riad, S., Philobbos, E., and Othman, A. 2001, Subsurface structures and sedimentary basins in the Nile Valley area as interpreted from gravity data. Egyptian Journal of Geology, 45, 681–712.

Parkhurst, D. and Appelo, C., 1999, User's guide to PHREEQC (version 2) – a computer program for speciation, batch-reaction, one-dimensional transport, and inverse geochemical calculations. Water-Resources Investigations Report p. 99–4259, US Geological Survey, Denver, 312 p.

Piper, A., 1944, A graphic procedure in the geochemical interpretation of water analysis. American Geophysical Union Transactions, 25, 914–923.

Rice, E.W., Barid, R.B., Eaton, A.D., and Clesceri, L.S., 2012, Standard methods for the examination of water and wastewater (22nd edition). American Public Health Association, American Water Works Association, Water Environmental Federation, Washington, DC, 1496 p.

 https://doi.org/10.1007/s12303-018-0039-7

RIGW (Research Institute of Groundwater), 1997, Hydrogeological map of Luxor area (Scale 1:100 000). Explanatory notes, 23 p.

Said, R. 1981, The Geological evolution of the River Nile. Springer-Verlag, New York, 151 p.

Sayed, S., 2004, Effect of the construction of Aswan High Dam on the groundwater in the area between Qena and Sohag, Nile Valley, Egypt. Ph.D. Thesis, Assiut University, Assiut, 220 p.

Schoeller, H., 1956, Géochimie des Eaux Souterraines: Application aux Eaux des Gisements de Pétrole. Revue du Institut Franais du Ptrole et Annales des Combustibles Liquides, Sociéteé des éditions Technip, Paris, 213 p.

Thivya, C., Chidambaram, S., Thilagavathi, R., Prasanna, M., Singaraja, C., Nepolian, M., and Sundararajan, M., 2014, Identification of the geochemical processes in groundwater by factor analysis in hard rock aquifers of Madurai District, South India. Arabian Journal of Geoscience, 7, 3767–3777.